East Clive, Hawkes Bay

Hastings Outfall Stage 2 Assessment

Report prepared for Hastings District Council

August 2020

Document History

Versions

Version	Revision Date	Summary	Reviewed by
0.1	19/7/2020	Draft for internal review	Goward Brown
0.2	20/7/2020	Draft for internal review	Berthot
0.3	23/7/2020	Draft for internal review	Goward Brown
0.4	26/7/2020	Draft for Client review	Berthot
0.5	16/7/2020	Revised Draft addressing Stantec Comments	Goward Brown
0.6	17/8/2020	Draft for Client review	Berthot
0.7	24/08/2020	Revised Draft addressing Stantec Comments	Goward Brown
0.8	25/08/2020	Draft for Client review	Berthot

Distribution

Version	Date	Distribution

Document ID:

Contents

List of Figures

List of Tables

1.Introduction

The Hastings District Council (HDC) operates the East Clive Wastewater Outfall, located to the northeast of the City of Hastings. The outfall (Figure 1.1) extends some 2750 m offshore and has 52 diffuser ports discharging in approximately 9 m of water depth (mean sea level). The treated effluent discharge flows range from 51,000 m^3 per day (average dry weather flow; ADWF) to 120,000 m^3 per day (peak wet weather flow; PWWF).

Previous hydrodynamic and diffusion modelling of the outfall was commissioned by HDC in 2009 and 2012. The report commissioned in 2010 explored the outfall plume dynamics under a range of expected environmental conditions to quantify bacterial, viral and suspended solids concentrations within the receiving coastal environment. A wave, wind and current hindcast model was developed covering regional and local scales to quantify the range of environmental conditions at the site. The hydraulics of the pipeline were quantified, and diffuser modelling was undertaken to provide boundary conditions for the lagrangian based model for the plume dynamics. The report commissioned in 2012 expanded this further to produce spatial maps of dilution statistics and generate a time-series of predicted dilutions at discrete monitoring locations.

After damage was sustained to three adjacent pipeline joints, HDC now require modelling to assess the risks associated with the complete failure of the damaged joints to feed into a condition assessment of the pipeline which is being undertaken by Stantec. The scope of work is to run three Lagrangian particle tracking model scenarios, using the open source lagrangian particle tracking model, OpenDrift. The scenarios assume a full flow leak at an average daily flow rate of 48,000 $m3.day^{-1}$ based on the existing effluent discharge data.

The three proposed scenarios are as below:

1. Scenario 1 assumes normal operation of dispersion at the end of the outflow (2750 m from the shore)
2. Scenario 2 assumes a flow occurring halfway along the pipe (1375 m from the shore)
3. Scenario 3 assumes a breach a quarter of a way from the shoreline (685 m from the shore).

The report is organised as follows: Section 2 provides a summary of the existing model data and a description of the particle-tracking model and its application to the plume dispersal scenarios simulated, Section 3 provides the results of the plume simulations. Section 4 gives a concise summary of the results presented in Section 3. Finally, Section 5 gives the references cited in this report.

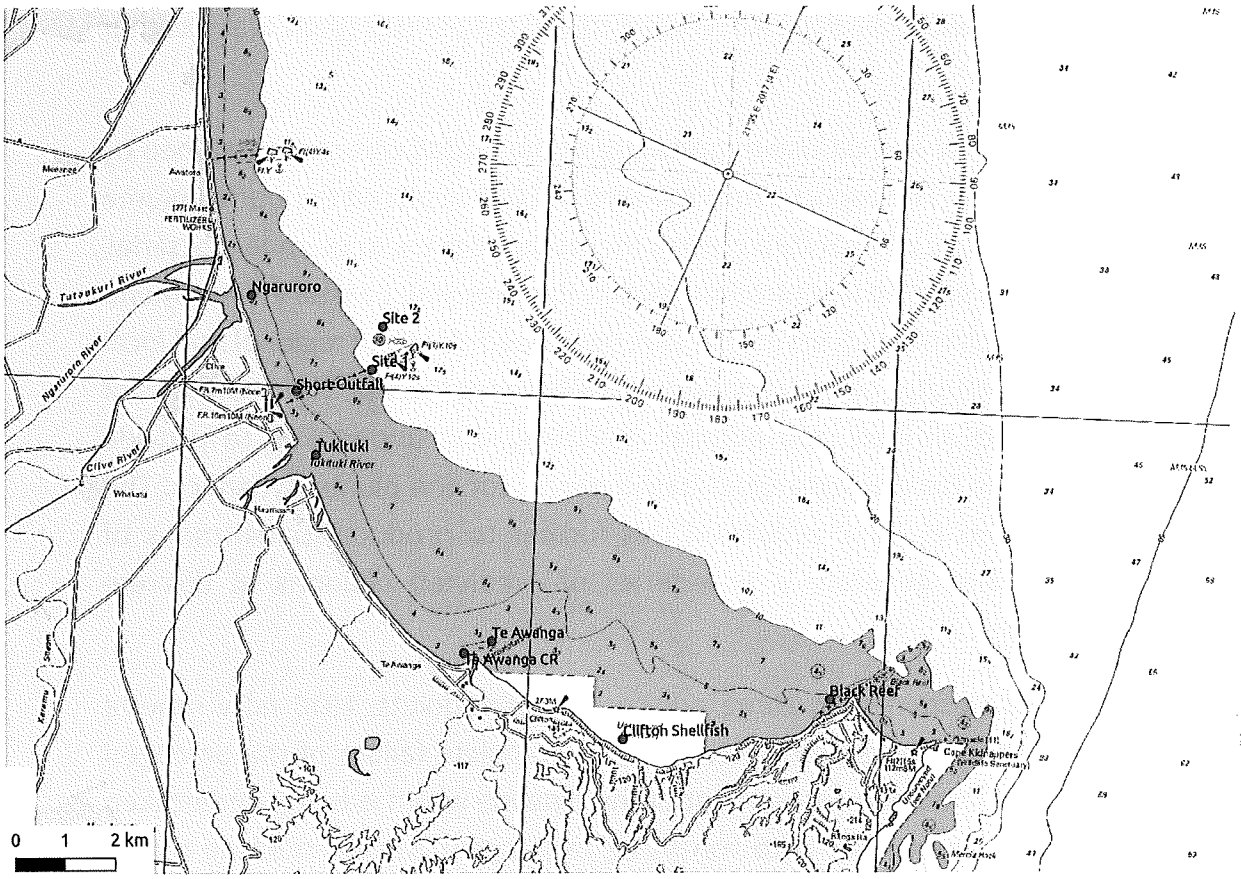

Figure 1.1 *Location of the East Clive Wastewater Outfall. Green points indicate the release locations for each scenario. The red circles show the locations where time series were extracted, given in Table 2.2.*

2. Methods

A full description of the 3D hydrodynamic model, SELFE, used to provide the 3-dimensional current and wind conditions for the Lagrangian particle tracking model are given in the previous MOS report (2010)[1]. From the previous studies, the transport and dispersion results from the previous MOS reports[1,2], showed similar results for both modelled El Niño and La Niña years. El Niño conditions tend to impose a west-southwest anomaly on the 'normal' wind conditions. For La Niña events, the opposite is generally true, and this results in an east-north-easterly wind field anomaly. Previous reporting (MOS, 2010) suggested that whilst directional distribution is not significantly altered between modelled scenarios, the El Niño year sees an increase in mean and median current speeds compared to the La Niña year, suggesting that El Niño will enable greater particle dispersion. The hydrodynamic model data used for these simulations was for June – July 2002 (an El Niño climatic regime).

2.1 Wastewater Plume Dispersion Modelling

2.1.1 OpenDrift Model description

The transport and dispersion of a conservative tracer was simulated using the ocean trajectory modelling framework OpenDrift[3] (Dagestad et al. 2018). OpenDrift is an open-source Python-based framework for Lagrangian particle tracking developed by the Norwegian Meteorological Institute, where it is notably used operationally as an emergency response tool for oil spill and search and rescue events. The framework is highly modular and can be used for any type of drift calculations in the ocean or atmosphere. Several modules have already been developed, including an oil drift module (see Röhrs et al., 2019), a stochastic search-and-rescue module, a pelagic egg

---

[1] MSL (2010). East Clive Wastewater Outfall Hydrodynamic modelling. Report prepared for Hasting District Council by MetOcean Solutions Ltd and Cawthron Institute.

[2] MSL (2012). East Clive Wastewater Outfall Dilution Statistics. Report prepared for Hasting District Council by MetOcean Solutions Ltd.

[3] https://github.com/OpenDrift/opendrift7

module, and a plastic drift module. The dispersion simulations described in the study were undertaken using the generic OceanDrift3D [4] module. The wastewater dispersion modelling consists of a trajectory tracking scheme applied to discrete particles in time and space-varying 3D oceanic currents (2.1):

$$\frac{dx_p}{dt} = \tilde{u}(x,y,z,t) + u_t$$

$$\frac{dy_p}{dt} = \tilde{v}(x,y,z,t) + v_t$$

$$\frac{dz_p}{dt} = w_t$$

(2.1)

where (xp, yp, zp) are particle 3D coordinates, $\tilde{u}(x,y,z,t), \tilde{v}(x,y,z,t)$ are horizontal ocean currents, u_t, v_t, w_t are the diffusion components representing turbulent motions.

In the horizontal plane, particles were advected by ocean currents using a 4th-order Runge-Kutta tracking scheme, and subject to additional displacement by horizontal diffusion. In the OpenDrift framework, the horizontal diffusion is included by applying an uncertainty to the horizontal current magnitudes. The magnitude of the current uncertainty was estimated using the general diffusion equation (2.2):

$$\int_t^{t+\Delta t} u_t \cdot d_t = \sqrt{6K_{u,v} \cdot \Delta t} \cdot \theta(-1,1)$$

(2.2)

where $\theta(-1,1)$ is a random number from a uniform distribution between -1 and 1, Δt is the time-step of the model in seconds and $K_{u,v}$ is the horizontal eddy diffusivity coefficient in $m^2 \cdot s^{-1}$.

In the vertical plane, particles are subject to diffusive displacement (w_t) due to vertical turbulent motion through the water column. In OpenDrift, the vertical mixing process is parameterised using a numerical scheme described in Visser (1997) which is similar

---

4 https://github.com/OpenDrift/opendrift/blob/master/opendrift/models/oceandrift3D.py

to equation 2.2 when using a constant vertical diffusion coefficient, Kz (as employed here).

Horizontal and vertical diffusion are included in the dispersion modelling to account for the mixing and diffusion caused by sub-grid scale turbulent processes, such as eddies, which are not explicitly resolved by the hydrodynamic models.

For dispersion at oceanic scales, Okubo (1974,1971) proposed that $K_{u,v}$ varies approximately as Equation 2.3a, close to the general 4/3 power law often considered for atmospheric (Richardson, L.F 1962) and oceanic diffusions (Batchelor, 1952; Stommel, 1949; Equation 2.3b):

$$k_{u,v} = 0.103 \cdot L^{1.15} \qquad (a)$$

$$k_{u,v} = \alpha \cdot L^{\frac{4}{3}} \qquad (b)$$

(2.3)

where L is the horizontal scale of the mixing phenomena and α indicates proportionality.

These equations relate the magnitude of the eddy diffusivity ($K_{u,v}$) to the length scale of the phenomena and this 4/3 power relationship was found to be applicable over a large range of scales (10 m to 1000 km) (Okubo 1974; Okubo, A. 1971). A similar relationship was found by List et al. (1990) in coastal waters.

In the present study, since high resolution flows are resolved, the amount of added diffusion should be limited. A generic horizontal coefficient of 0.01 $m^2 s^{-1}$ was applied which is consistent with a length scale of the order 20 - 40 m. The spatial scales of the vertical turbulent motions within the water column are one or several orders of magnitude smaller than horizontal turbulence. The vertical diffusion coefficient was set to a value of 1 $cm^2 s^{-1}$.

Particles are released continuously over a month and are given a further 14 days to disperse after the final release. In addition, the particles are each given a maximum age of 30 days which prevents a build-up of particles towards the end of the simulation; The particles are assumed to be passive (neutrally buoyant with no decay and to facilitate comparison between each three release locations), and are released randomly over the full depth of the water column. In terms of dispersion within the nearfield, the jet trajectory is assumed to be dominated by the momentum of the discharge from the pipe (Zhao, Chen, and Lee 2011). Distributing the particles

randomly across the water column enables further spread of the particles and reduces the possibility that the particles will become trapped on the seabed next to the release location. For scenario 1: The 'normal' operation scenario, particles are given additional randomness to their starting positions through horizontal distribution over a radius of 10 m. This simulates the additional, and initial, dispersion provided by the diffusers at the end of the outflow.

An average daily flow rate has been assumed to be 48,000 m^3 day^{-1} for all three scenarios. Time series of the concentrations are extracted from the model every half an hour over a month, to capture tidal variation in the signal.

Statistical maps of dilution are produced from the particle distribution at each output timestep of the particle tracking model; the dilution fields can be scaled to any reference concentration (e.g. $mg.L^{-1}$, $cfu.L^{-1}$, $pfu.L^{-1}$) to obtain absolute results. The particle distribution is obtained by generating a grid with the smallest grid size as is computationally practical, in this case, grid cells were 20 m by 20 m.

The normalized depth-averaged tracer concentration is obtained by a) computing the particle concentration at each cell (numbers of particles divided by cell volume), and b) normalizing by the nearfield particle concentration at the discharge location. This normalized tracer concentration quantifies the spatial relative dilution of the concentration near the discharge location (nearfield concentration).

A nominated nearfield concentration of 1 $mg.L^{-1}$was assumed to enable specific contaminant levels to be determined using concentration ratios. Based on this, a concentration of 0.001 $mg.L^{-1}$ is equivalent to a dilution factor of 1000, while a concentration level of 0.01 $mg.L^{-1}$ is equivalent to a dilution factor of 100.

In order to compare between the three scenarios, the outflow remains constant, as a result we would expect the dilutions extrema to be more conservative than in the previous MOS reports. Using the plume footprints, it will be possible to assess the impact of a breach closer to the nearshore region compared to normal operation.

2.1.2 Modelling Scenarios

Three scenarios are simulated (Table 2.1) and the results are presented in the form of time series of concentrations at a number of locations (see Table 2.2), and as statistical maps.

Table 2.1 Summary of Scenarios

Scenarios	Longitude	Latitude	Flowrate [m3/day]
Normal -End of Outflow Pipe	176.965	-39.5778	48 000
½ length of pipe	176.953	-39.582	48 000
¼ length of pipe (from the shore)	176.9467	-39.5842	48 000

Table 2.2 Description of the sites from which time series of concentration are extracted within the model domain (Figure 1.1)

	Site description and location		
	Latitude (° S)	**Longitude (° E)**	**Water Depth (m)**
Black Reef	39.6362	177.0708	5.00
Clifton Shellfish	39.6450	177.0228	2.00
Ngaruroro	39.5672	176.9314	2.50
Short Outfall	39.5842	176.9428	5.00
Te Awanga	39.6282	176.9911	2.00
Te Awanga CR	39.6306	176.9847	1.00
Tukituki	39.5957	176.948	1.00
Site 1	39.5798	176.9604	10.00
Site 2	39.5719	176.9625	10.00

3. Results

This section of the report presents results from a month-long particle tracking simulation, during June-July 2002. The dispersion modelling results presented below show the expected dilution and concentration of tracers for the following scenarios: 'Normal Outflow Operation', a flow halfway along the length of the pipe and at a quarter of the outfall length from the shore (Scenarios 1, 2 and 3 respectively). The daily average flow rate was kept constant to facilitate comparison between the scenarios.

The dilution maps (Figure 3.11-Figure 3.16) and levels can be interpreted in terms of relative concentration, where a dilution factor of 1000 is the equivalent of $1e^{-3}$ $X.L^{-1}$, while a dilution factor of 100 is equivalent to a concentration level of $1e^{-2}$ $X.L^{-1}$ (where X is represents an arbitrary unit of concentration measurement).

Note, the results in Figure 3.11 -Figure 3.16 are given on a logarithmic scale (base 10) due to the localised nature of the peaks in the data. Enlarged versions of Figure 3.11 to Figure 3.16 are given in Appendix A (Figure A. 1 to Figure A. 6).

Time-series of tracer concentration (assuming a concentration of 1 $mg.L^{-1}$) were extracted at several sites within the model domain (Figure 1.1). These sites cover the edge of near field region, shellfish sites, contact, fishing and boating recreation sites (Table 2.2). Statistical analysis of the time series comparing each of the three scenarios is presented for each of the extraction locations in Table 3.1 to Table 3.9. Presented are the maximum and mean values and the time taken for concentrations to reach, or exceed, these values, calculated from the start of the simulation.

From the extracted time-series histograms displaying the number of events which occur for different dilution thresholds (between 1 and 10000, split into 100 bins) are generated for each site and presented in Figure 3.2 to Figure 3.10.

In the present application, several sites are in shallow water (<10 m) and can even be dry at times. The result is that division by the water depth in the volume calculation can therefore result in artificial tracer spikes during periods of low water levels. Therefore, caution is advised during interpretation of tracer concentration at the shallowest of sites (notably Tukituki and Te Awanga CR).

As with the time series results, care should be taken when considering the particle counts in shallow water regions in Figure 3.1-Figure 3.6, as elevated particle accounts can occur in regions of shallow water where:

- Resident times of particles can be relatively long due to comparatively quiescent conditions resulting in higher concentrations when averaged over time
- Small fluctuations within the intertidal areas may maintain elevated levels of tracer due to the inability of the areas to effectively flush
- The process of converting the particle distributions to a volume will result in apparent elevation of concentrations in shallow water. To counter this, water depths shallower than 1m are masked out.

Table 3.1 Statistics derived from the time series extracted at Black Reef for each of the three scenarios

Statistics	Scenario 1	Scenario 2	Scenario 3
Maximum [mg.L^{-1}]	0.0005	0.000884	0.000306
Time taken to reach maximum [days]	18.729	17.125	1.8125
Mean [mg.L^{-1}]	7.10E-07	5.02E-06	1.74E-06
Time taken to reach mean [days]	18.729	1.229	1.812

Table 3.2 Statistics derived from the time series extracted at Clifton Shellfish for each of the three scenarios

Statistics	Scenario 1	Scenario 2	Scenario 3
Maximum [mg.L^{-1}]	0.001267	0.00112	0.001289
Time taken to reach maximum [days]	34	14.438	40.979
Mean [mg.L^{-1}]	6.00E-07	6.89E-06	8.85E-06
Time taken to reach mean [days]	34	14.438	5.208

Table 3.3 Statistics derived from the time series extracted at Ngaruroro for each of the three scenarios

Statistics	Scenario 1	Scenario 2	Scenario 3
Maximum [mg.L^{-1}]	0.001018	0.001737	0.001504
Time taken to reach maximum [days]	16.917	42.042	42.042
Mean [mg.L^{-1}]	2.89E-06	4.11E-06	1.19E-05
Time taken to reach mean [days]	16.917	21.646	14.354

Table 3.4 Statistics derived from the time series extracted at Short Outfall for each of the three scenarios

Statistics	Scenario 1	Scenario 2	Scenario 3
Maximum [mg.L^{-1}]	0.0005	0.000442	0.001018
Time taken to reach maximum [days]	22.771	14.583	19.208
Mean [mg.L^{-1}]	1.18E-06	2.30E-06	7.71E-06
Time taken to reach mean [days]	22.771	14.583	3.666

Table 3.5 Statistics derived from the time series extracted at Tukituki for each of the three scenarios

Statistics	Scenario 1	Scenario 2	Scenario 3
Maximum [mg.L^{-1}]	0.001264	0.001131	0.001298
Time taken to reach maximum [days]	43.146	14.875	4.063
Mean [mg.L^{-1}]	5.98E-07	4.82E-06	1.50E-05
Time taken to reach mean [days]	43.146	14.875	3.583

Table 3.6 Statistics derived from the time series extracted at Site 1 for each of the three scenarios

Statistics	Scenario 1	Scenario 2	Scenario 3
Maximum [mg.L^{-1}]	0.00075	0.000442	0.000254
Time taken to reach maximum [days]	23.958	22.104	22.937
Mean [mg.L^{-1}]	5.80E-06	4.08E-06	7.83E-07
Time taken to reach mean [days]	15.75	11.625	6.291

Table 3.7 Statistics derived from the time series extracted at Site 2 for each of the three scenarios

Statistics	Scenario 1	Scenario 2	Scenario 3
Maximum [mg.L^{-1}]	0.00025	0.000221	0.000254
Time taken to reach maximum [days]	6.792	6.604	22.5
Mean [mg.L^{-1}]	4.85E-06	2.72E-06	1.45E-06
Time taken to reach mean [days]	6.791	6.604	6.729

Table 3.8 Statistics derived from the time series extracted at Te Awanga CR for each of the three scenarios

Statistics	Scenario 1	Scenario 2	Scenario 3
Maximum [mg.L^{-1}]	0.002666	0.002049	0.003717
Time taken to reach maximum [days]	23.687	15.729	41.458
Mean [mg.L^{-1}]	1.26E-06	9.70E-06	1.41E-05
Time taken to reach mean [days]	23.687	15.729	3.562

Table 3.9 Statistics derived from the time series extracted at Te Awanga for each of the three scenarios

Statistics	Scenario 1	Scenario 2	Scenario 3
Maximum [mg.L^{-1}]	0.001355	0.001201	0.000693
Time taken to reach maximum [days]	17.52083	4.583333	1.083333
Mean [mg.L^{-1}]	1.28E-06	3.98E-06	9.51E-06
Time taken to reach mean [days]	17.52083	4.583333	1.083333

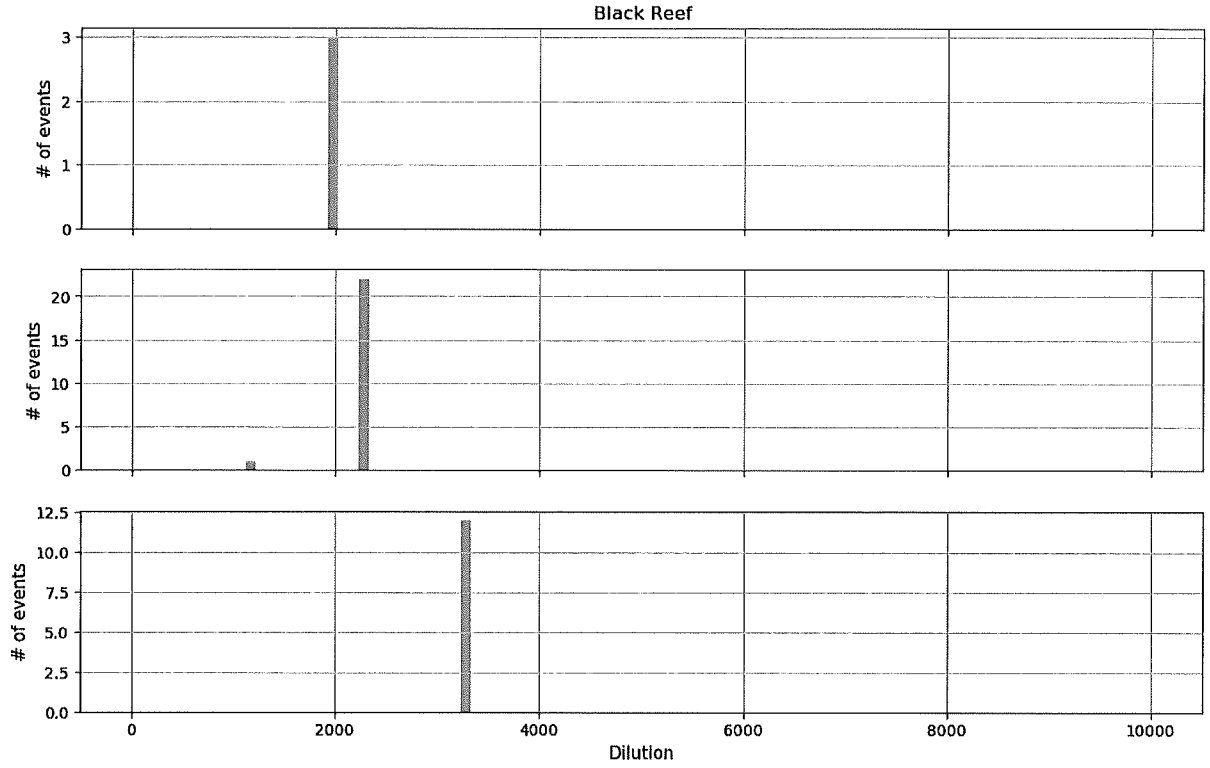

Figure 3.1 *Histograms of predicted dilutions at Black Reef for the 'Normal' scenario (top), the halfway along the length of the pipe scenario (middle) and the quarter of the length of the outflow scenario (bottom).*

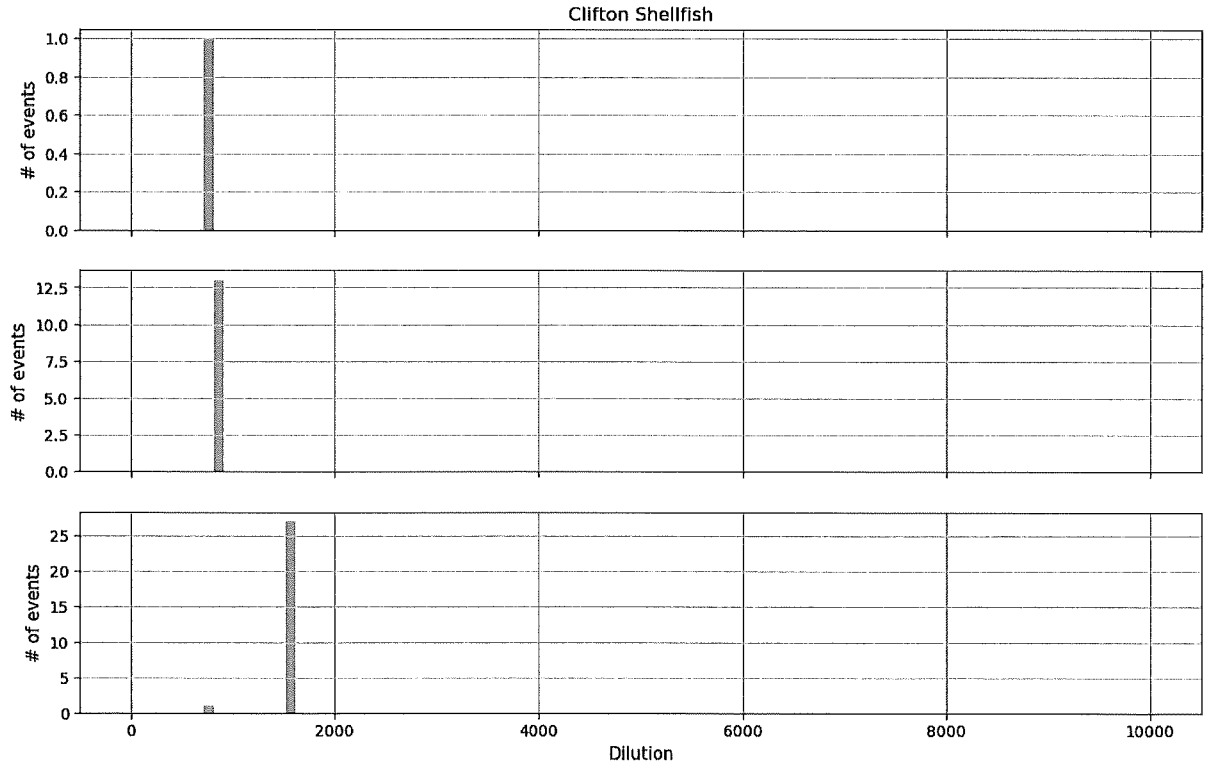

Figure 3.2 *Histograms of predicted dilutions at Clifton Shellfish for the 'Normal' scenario (top), the halfway along the length of the pipe scenario (middle) and the quarter of the length of the outflow scenario (bottom).*

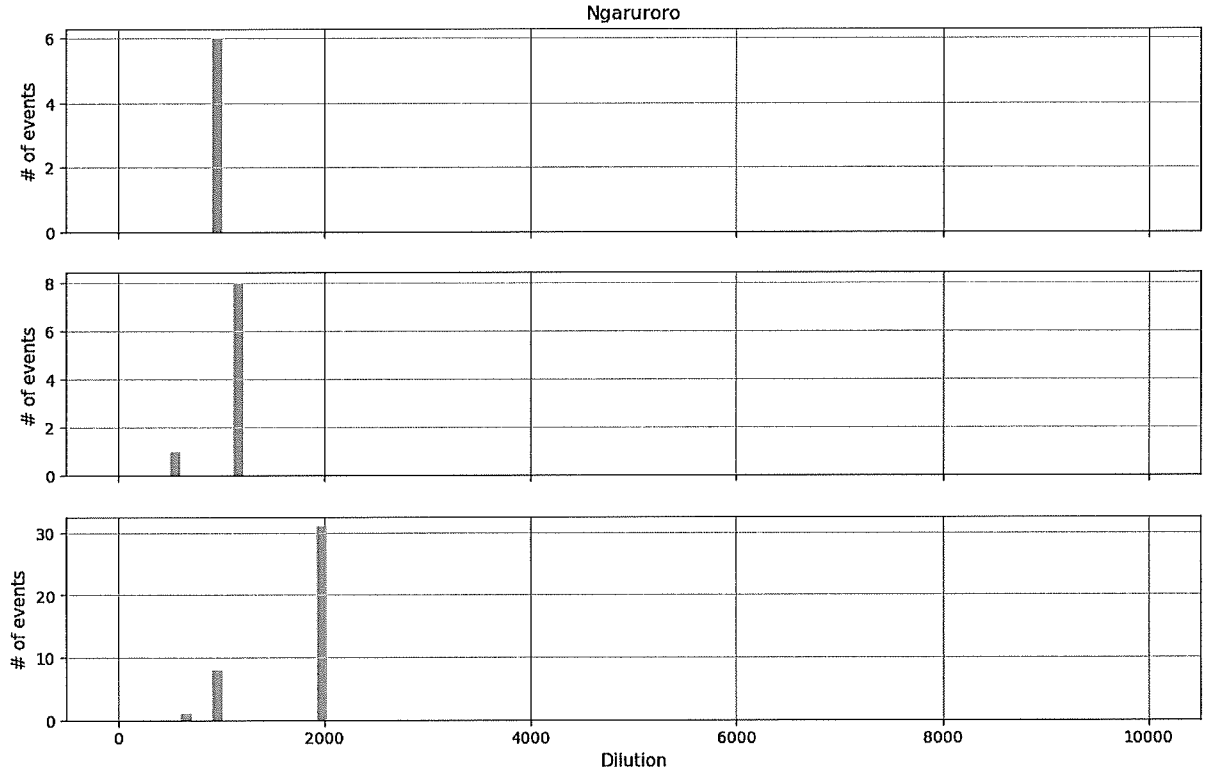

Figure 3.3 Histograms of predicted dilutions at Ngaruroro for the 'Normal' scenario (top), the halfway along the length of the pipe scenario (middle) and the quarter of the length of the outflow scenario (bottom).

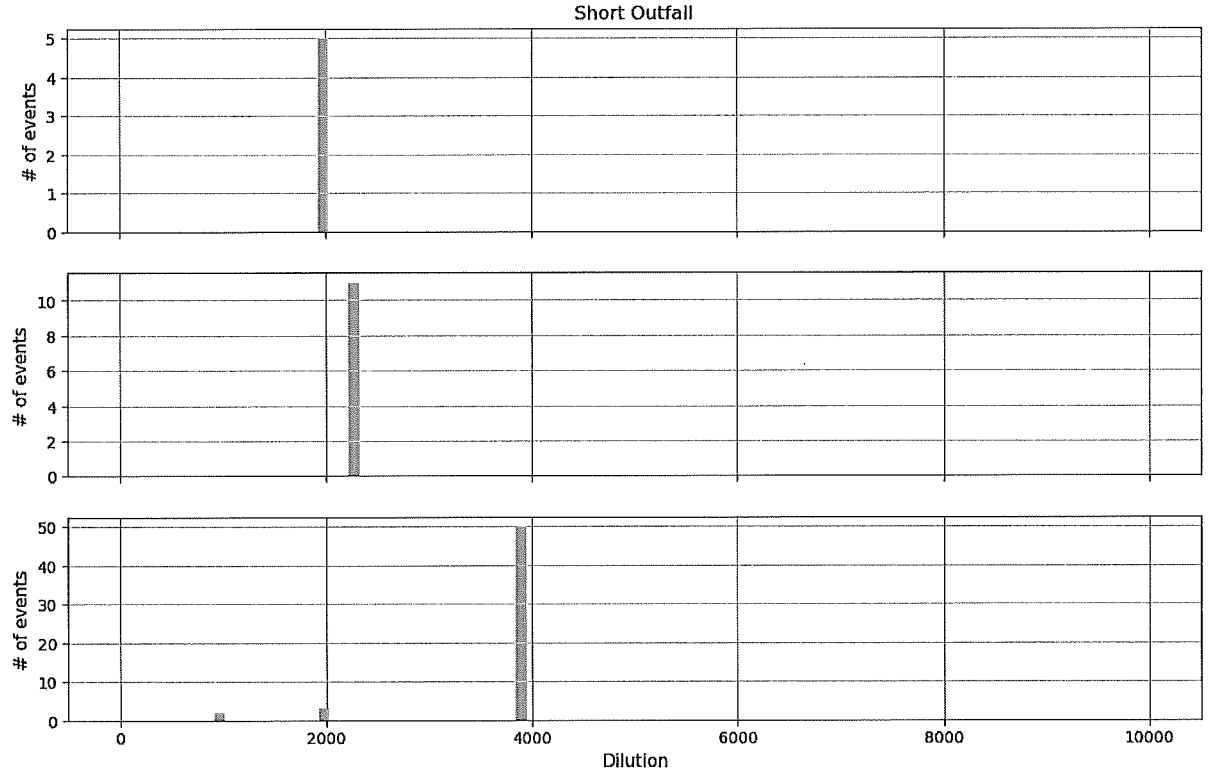

Figure 3.4 Histograms of predicted dilutions at Short Outfall for the 'Normal' scenario (top), the halfway along the length of the pipe scenario (middle) and the quarter of the length of the outflow scenario (bottom).

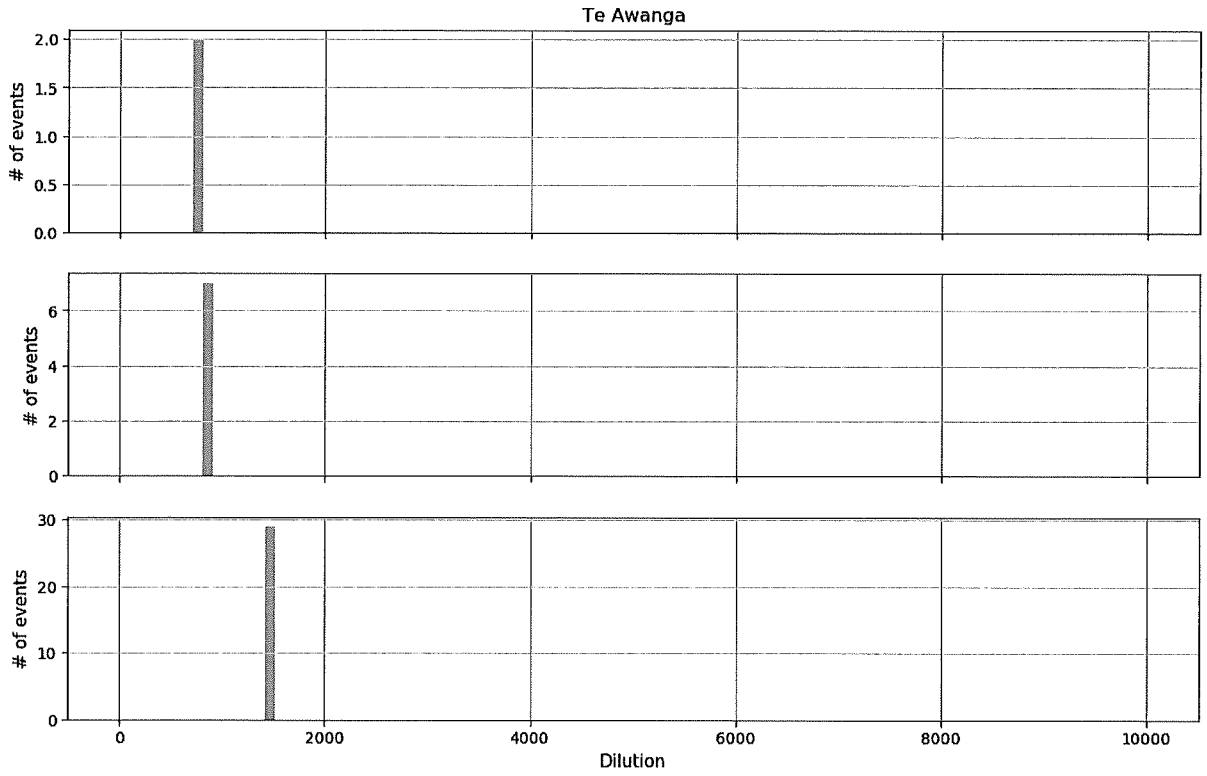

Figure 3.5 *Histograms of predicted dilutions at Te Awanga for the 'Normal' scenario (top), the halfway along the length of the pipe scenario (middle) and the quarter of the length of the outflow scenario (bottom).*

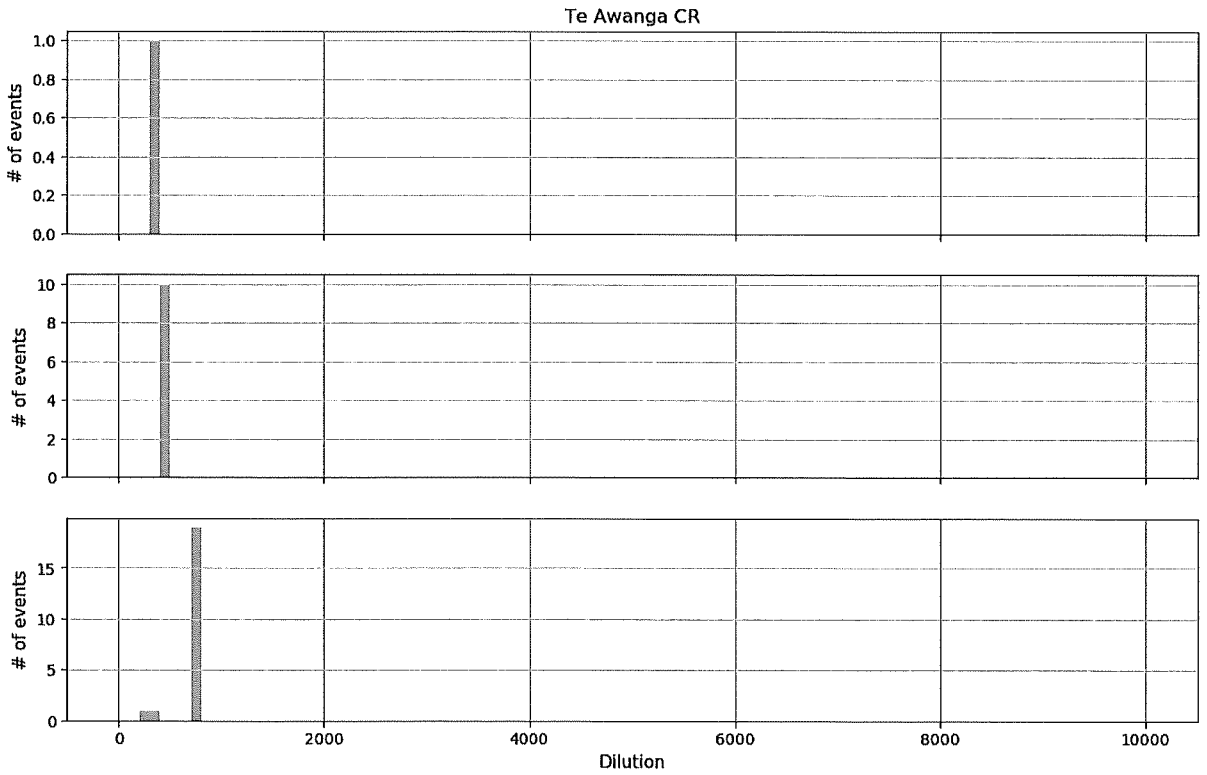

Figure 3.6 *Histograms of predicted dilutions at Te Awanga CR for the 'Normal' scenario (top), the halfway along the length of the pipe scenario (middle) and the quarter of the length of the outflow scenario (bottom).*

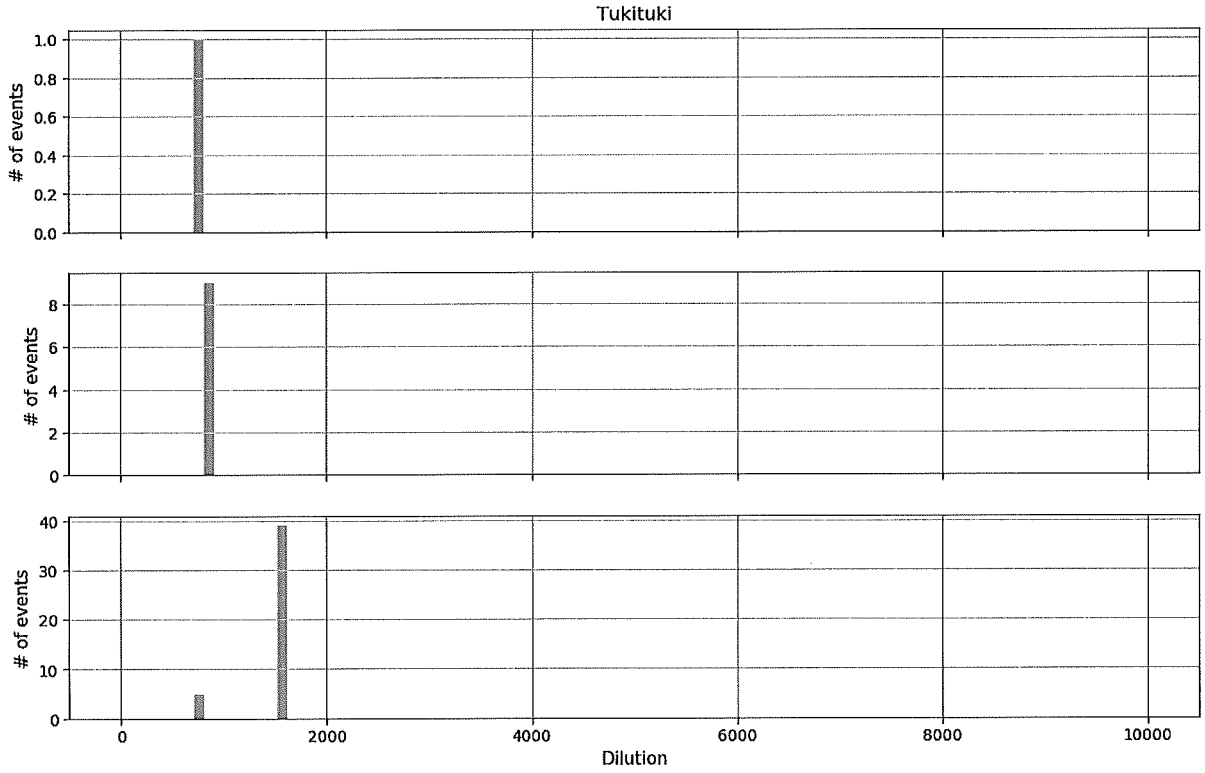

Figure 3.7 *Histograms of predicted dilutions at Tukituki for the 'Normal' scenario (top), the halfway along the length of the pipe scenario (middle) and the quarter of the length of the outflow scenario (bottom).*

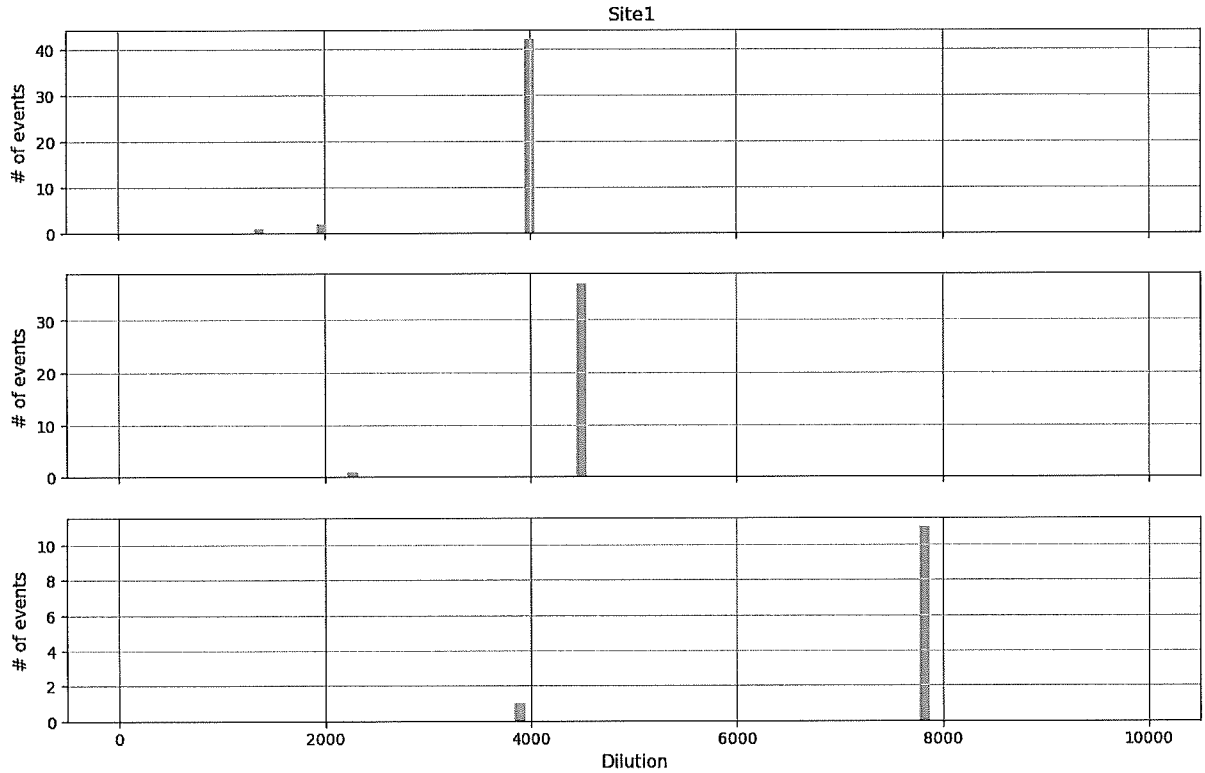

Figure 3.8 *Histograms of predicted dilutions at Site 1 for the 'Normal' scenario (top), the halfway along the length of the pipe scenario (middle) and the quarter of the length of the outflow scenario (bottom).*

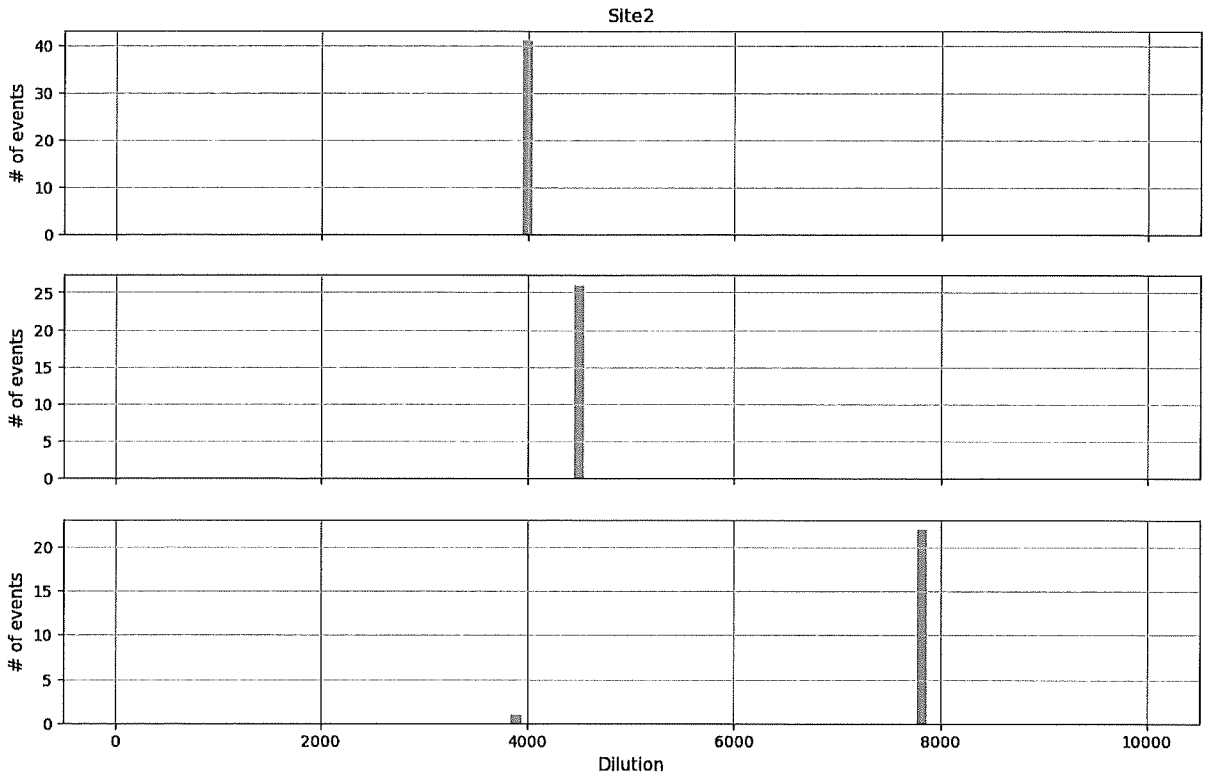

Figure 3.9 *Histograms of predicted dilutions at Site 2 for the 'Normal' scenario (top), the halfway along the length of the pipe scenario (middle) and the quarter of the length of the outflow scenario (bottom).*

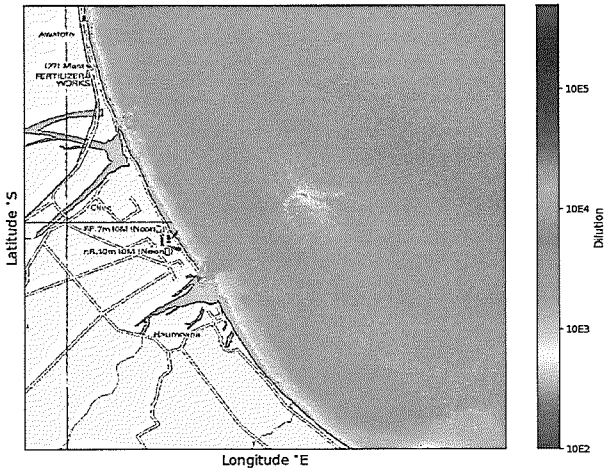

Figure 3.10 Maximum dilution during a month-long release at a rate of 48,000 m 3 day-1 for the 'normal' operation scenario. Dilutions above 5.10^5 have been masked.

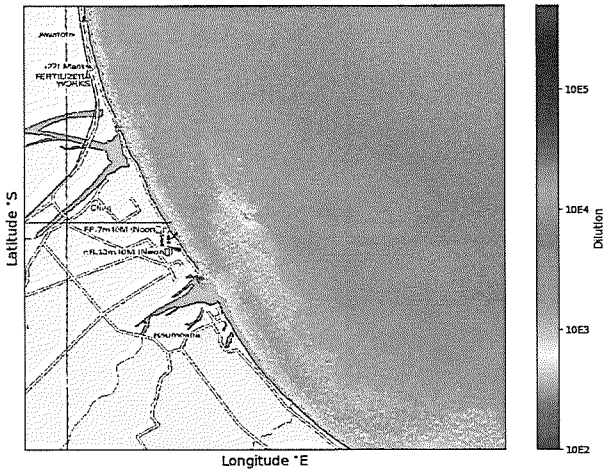

Figure 3.11 Maximum dilution during a month-long release at a rate of 48,000 m3 day1 for a pipe break halfway along the pipe. Dilutions above 5.10^5 have been masked.

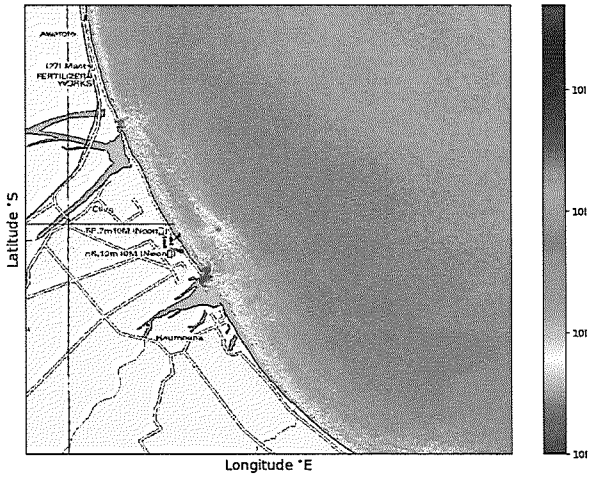

Figure 3.12 Maximum dilution during a month-long release at a rate of 48,000 m3 day-1 for a pipe break a quarter of the way along the pipe. Dilutions above 5.10^5 have been masked.

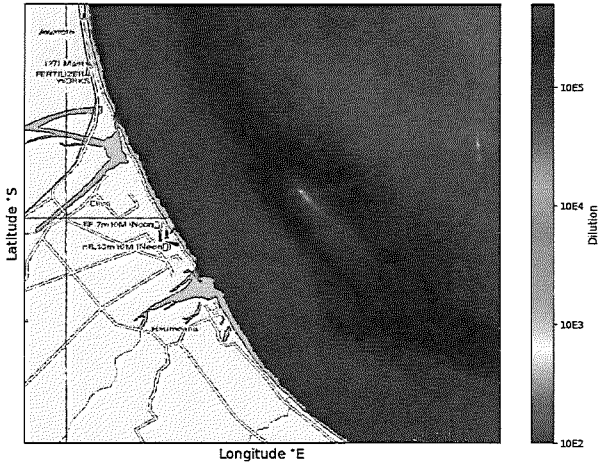

Figure 3.13 Mean dilution during a month-long release at a rate of 48,000 m 3 day-1 for the 'normal' operation scenario. Dilutions above 5.10^5 have been masked.

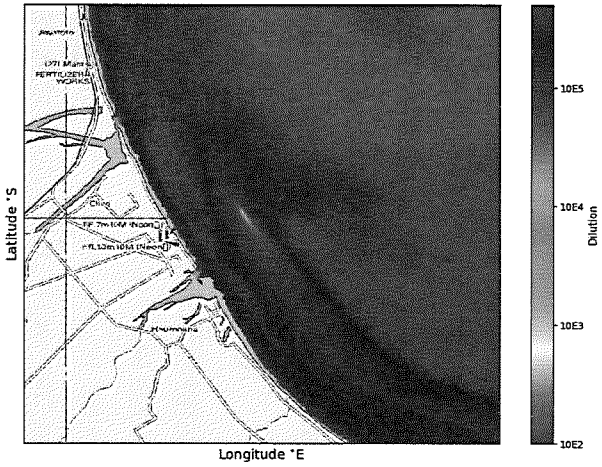

Figure 3.14 Mean dilution during a month-long release at a rate of 48,000 m 3 day-1 for a pipe break halfway along the pipe. Dilutions above 5.10^5 have been masked.

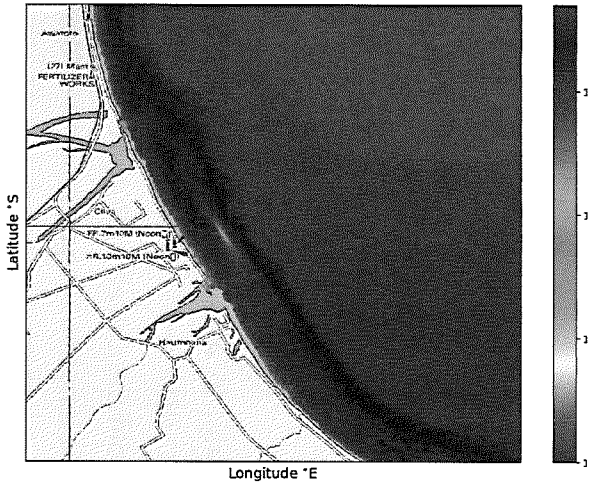

Figure 3.15 Mean dilution during a month-long release at a rate of 48,000 m3 day-1 for a pipe break a quarter of the way along the pipe. Dilutions above 5.10^5 have been masked.

4.Summary

Lagrangian tracer simulations have been undertaken to investigate the dispersion of water discharged from the East Clive Wastewater Outfall, from both normal operation and discharge due to a leak along the pipe. Three different scenarios were considered: 'Normal Outflow Operation', a flow halfway along the length of the pipe and at a quarter of the outfall length from the shore. Results were postprocessed in terms of dilution, giving flexibility to the user to apply a reference concentration.

The maximum dilution maps show the peak pollutant accumulation during 30 days of release for each location. The pipe break closest to the shore (scenario 3) has the greatest impact within the coastal area. Although the values in the shallow water regions should be considered with caution, there are accumulations of particles around the river mouths and along the coast. A pipe break at half the length of the outfall, sees a reduction in the spatial extent of plume and coastline affected. "Normal" operation shows the minimal amount of coastal impact.

The mean dilution maps illustrate how the plume footprint typically spreads south-west from the discharge location, consistent with the previous MOS reports. Dilutions can be converted into concentrations and the particles scaled to link to the consent. A key comparison between the previous MOS reports and the work presented here, is the change in extent of the plume relative to the release location. We see a greater plume footprint for the release closer to the shore than we do for the normal release where the particles experience more dispersion which suggests higher concentrations of pollutants will be found at greater distance from the source.

The concentration timeseries, assuming a concentration of 1mg.L^{-1} per particle, reflect the results shown in the spatial distribution statistical maps, with more sites receiving higher concentrations of the tracer during scenario 3. During "normal" operations (scenario 1), locations further afield (i.e Black Reef), infrequently receive raised levels (~0.0005 mg.L^{-1}) of tracer, and do so towards the end of the simulation, when the particles have had more time to disperse, compared to peak values of 0.0003 mg.L-1 during the nearshore release, scenario 3 which took 1.81 days to reach. Where the particles are released closer to the shore, all sites see more frequent peaks, although similar levels of tracer concentration are observed, with increasing frequency between scenarios 2 and 3.

The number of peak events at each site increases as the particles are released closer to the shore and indicates the greater likelihood of pollutant spikes reaching these locations than for the 'normal operation' scenario (scenario 1).

The exception to this are the offshore sites: 1 and 2, which are affected similarly for all cases.

5.References

Batchelor, G.K. 1952. "Diffusion in a Field of Homogeneous Turbulence. II. The Relative Motion of Particles." *Cambridge Philosophical Society*, no. 48: 345–62.

Dagestad, Knut-Frode, Johannes Röhrs, Øyvind Breivik, and Bjørn Ådlandsvik. 2018. "OpenDrift v1.0: A Generic Framework for Trajectory Modelling." *Geoscientific Model Development* 11 (4): 1405–20. https://doi.org/10.5194/gmd-11-1405-2018.

List, E., G. Gartrell, and C. Winant. 1990. "Diffusion and Dispersion in Coastal Waters." *Journal of Hydraulic Engineering.,* 116(10): 1158–79.

Okubo. 1974. "Some Speculations on Oceanic Diffusion Diagrams." *Rapports et Procès-Verbaux Des Reunions Du Conseil Permanent International Pour l'Exploration de La Mer.*

Okubo, A. 1971. "Oceanic Diffusion Diagrams." *Deep-Sea Research* 18: 789–802.

Richardson, L.F. 1962. "Atmospheric Diffusion Shown on a Distance Neighbour Graph." *Proc. R. Soc. London,* Ser A, (110): 709-737.

Röhrs et al. 2019. "The Effect of Vertical Mixing on the Horizontal Drift of Oil Spills." *Ocean Science* 14: 1581–1601.

Stommel, H. 1949. "Horizontal Diffusion Due to Oceanic Turbulence." *Journal of Marine Research*, no. 8: 199–225.

Visser A. 1997. "Using Random Walk Models to Simulate the Vertical Dis-." *Marine Ecology-Progress Series*, no. 158: 275–281.

Zhao, Chen, and Lee. 2011. "Modelling the Dispersion of Wastewater Discharges from Offshore Outfalls: A Review." *Environmental Reviews* 19 (1): 107–20.

Appendix A:

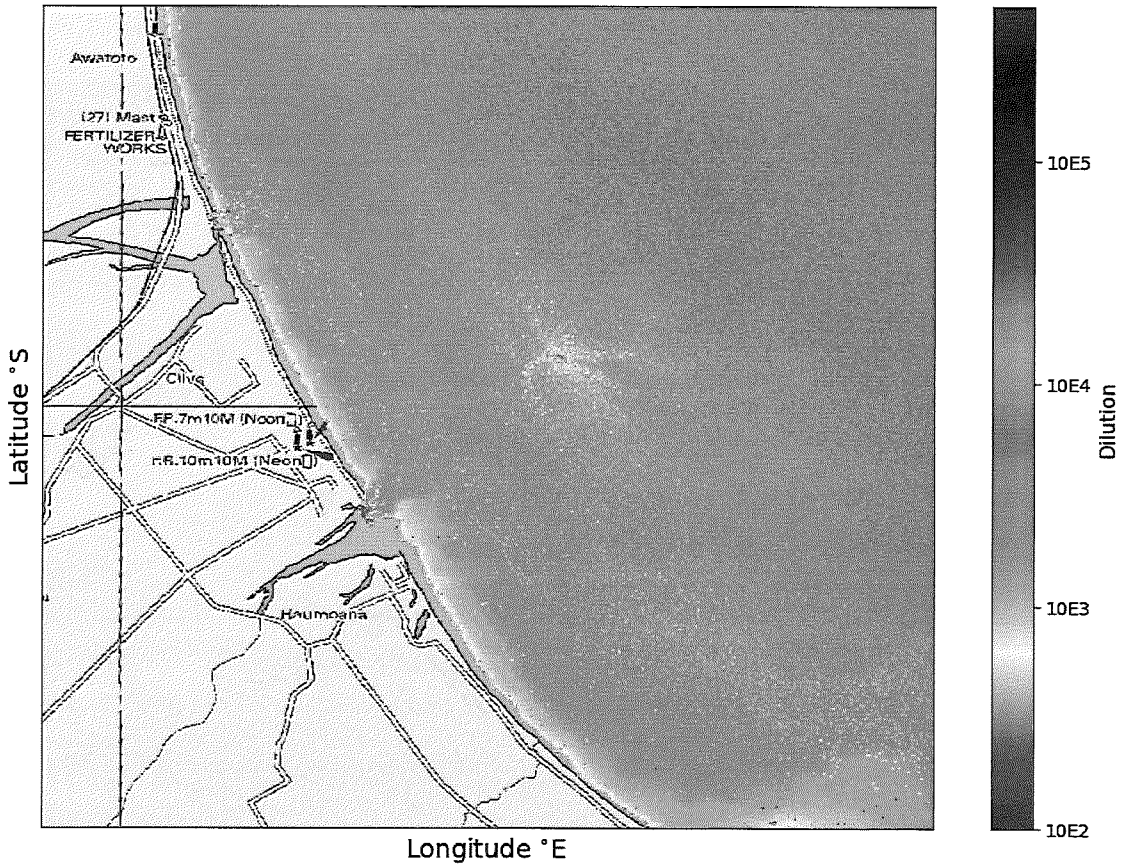

Figure A. 1 Maximum dilution during a month-long release at a rate of 48,000 m 3 day-1 for the 'normal' operation scenario. Dilutions above 5.10^5 have been masked.

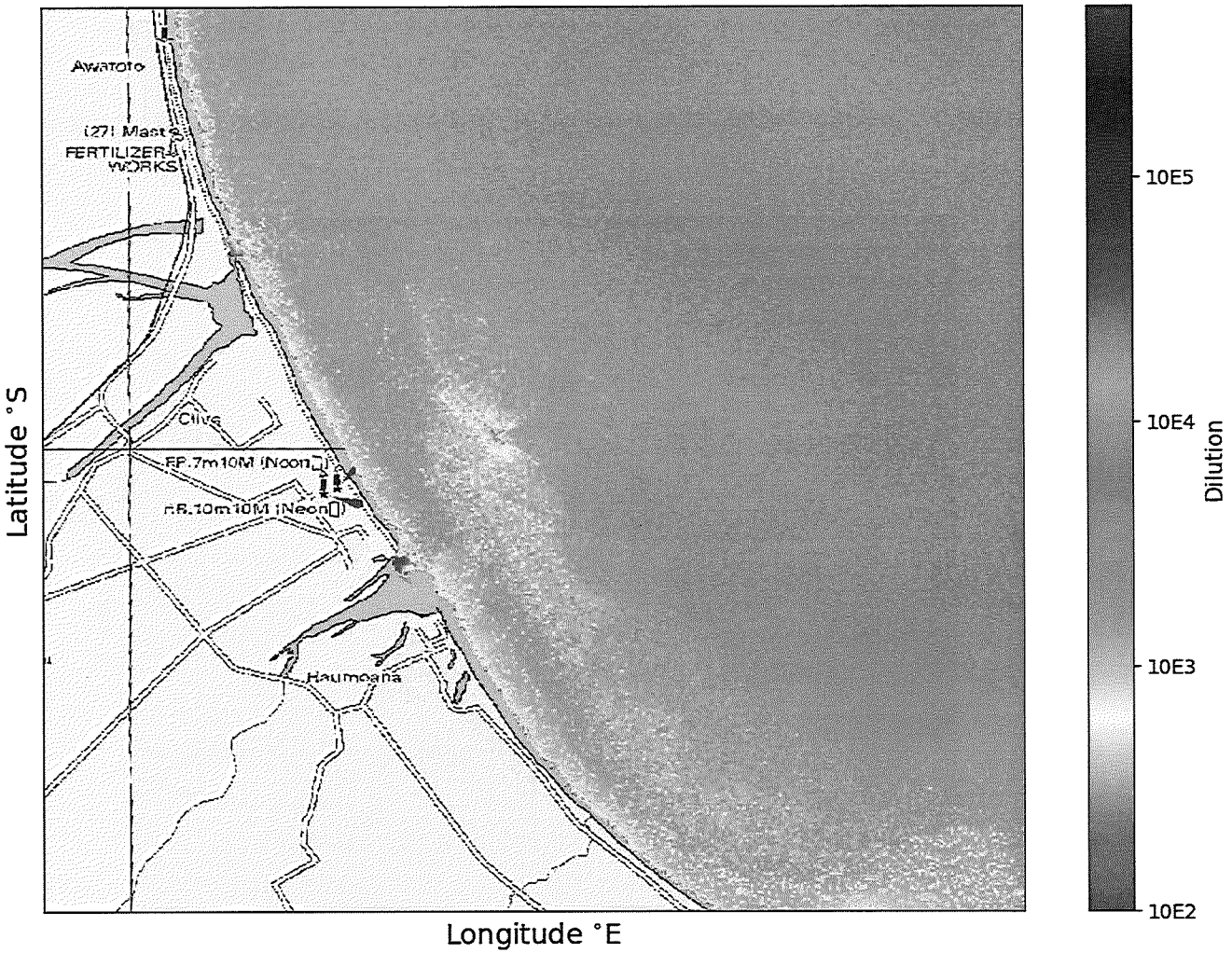

Figure A. 2 Maximum dilution during a month-long release at a rate of 48,000 m^3 day^1 for a pipe break halfway along the pipe. Dilutions above 5.10^5 have been masked.

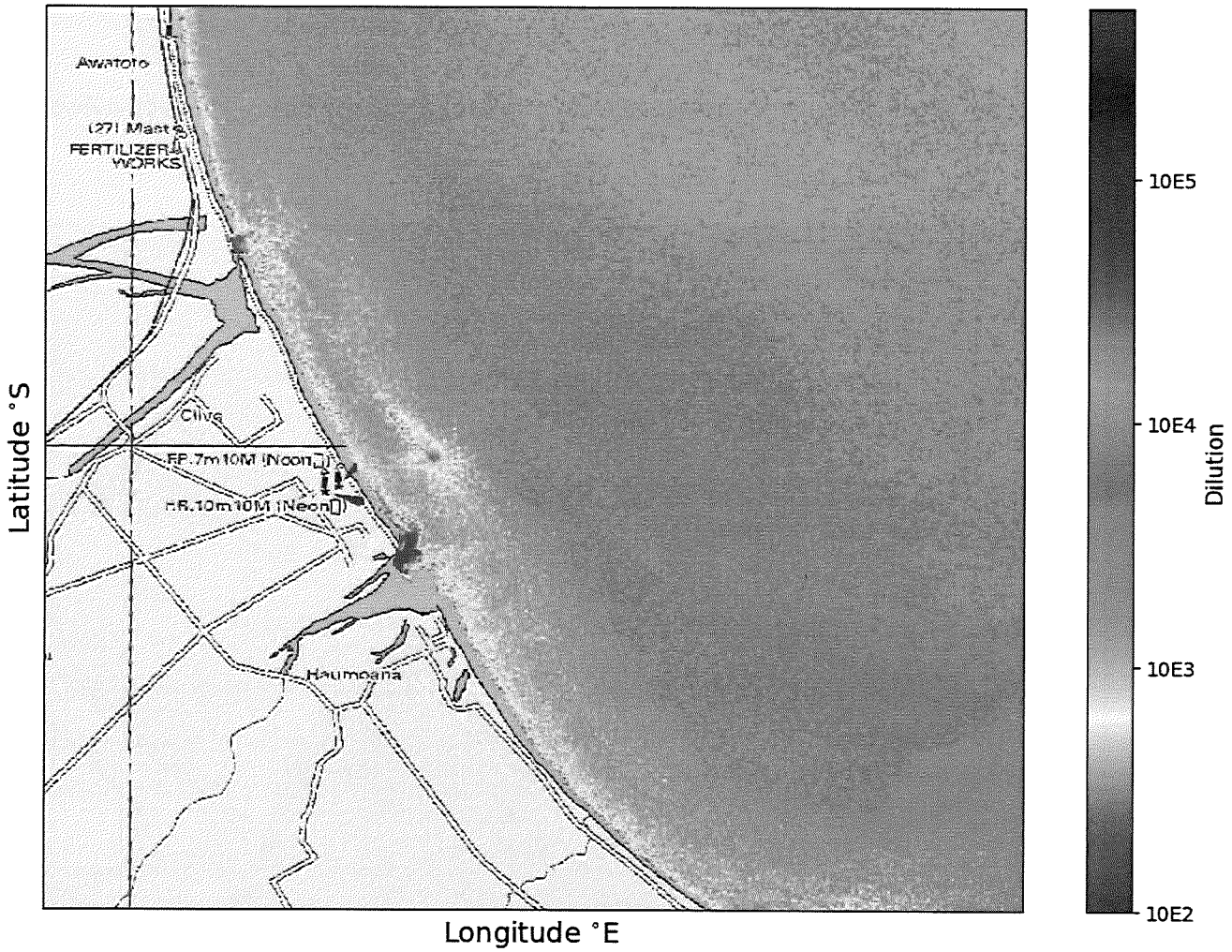

Figure A. 3 *Maximum dilution during a month-long release at a rate of 48,000 m3 day-1 for a pipe break a quarter of the way along the pipe. Dilutions above 5.10^5 have been masked.*

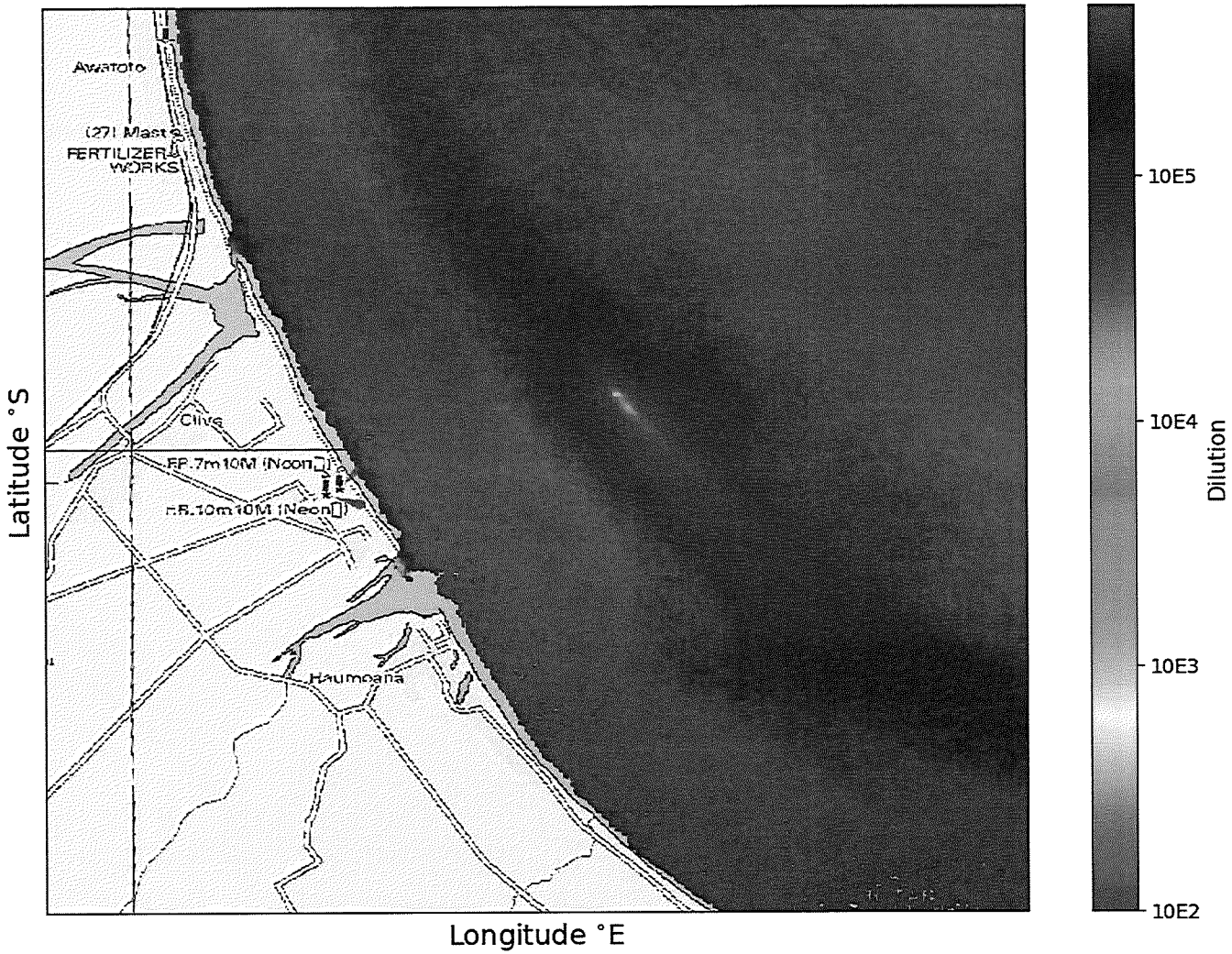

Figure A. 4 Mean dilution during a month-long release at a rate of 48,000 m 3 day-1 for the 'normal' operation scenario. Dilutions above 5.10^5 have been masked.

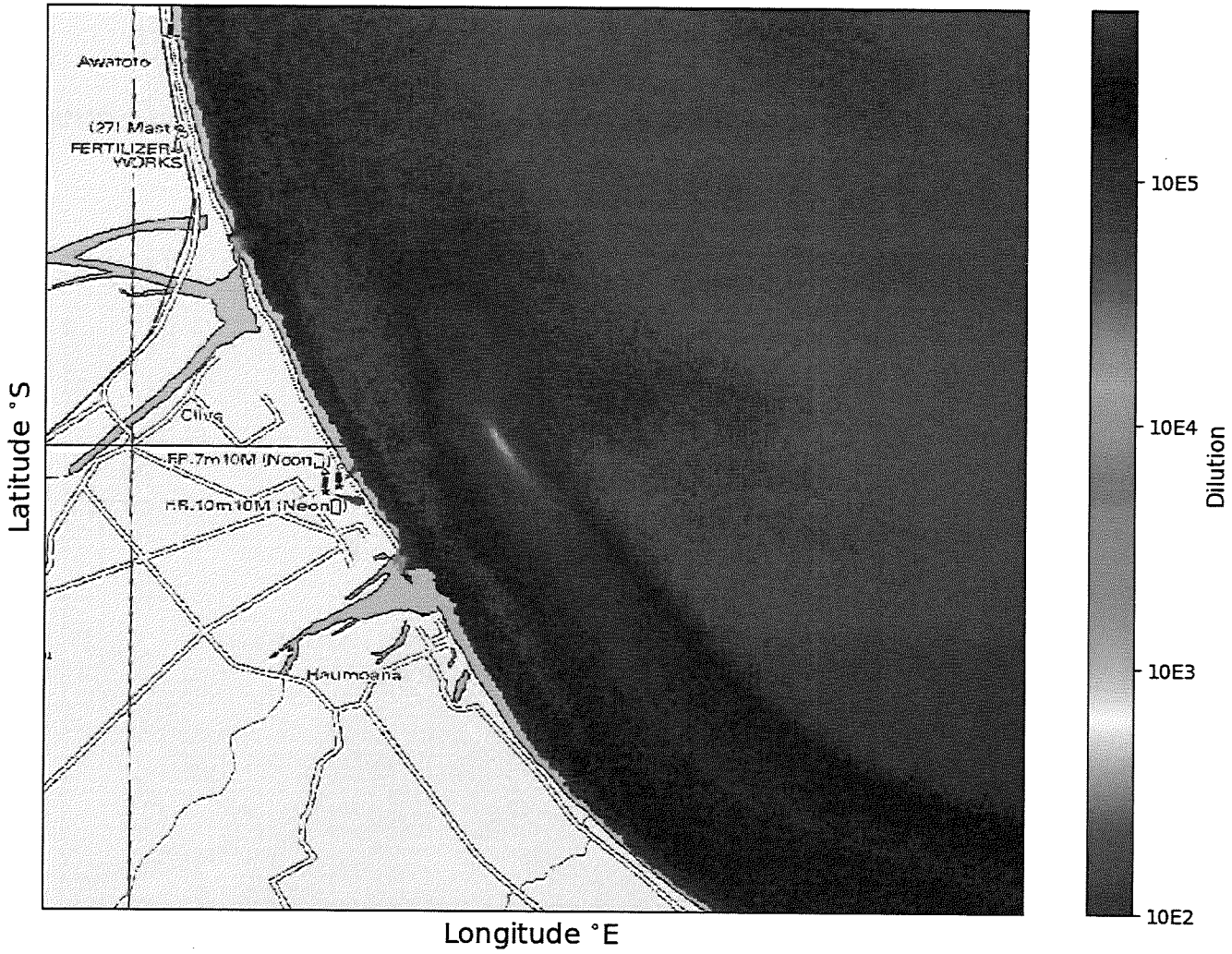

Figure A. 5 Mean dilution during a month-long release at a rate of 48,000 m 3 day-1 for a pipe break halfway along the pipe. Dilutions above 5.10^5 have been masked.

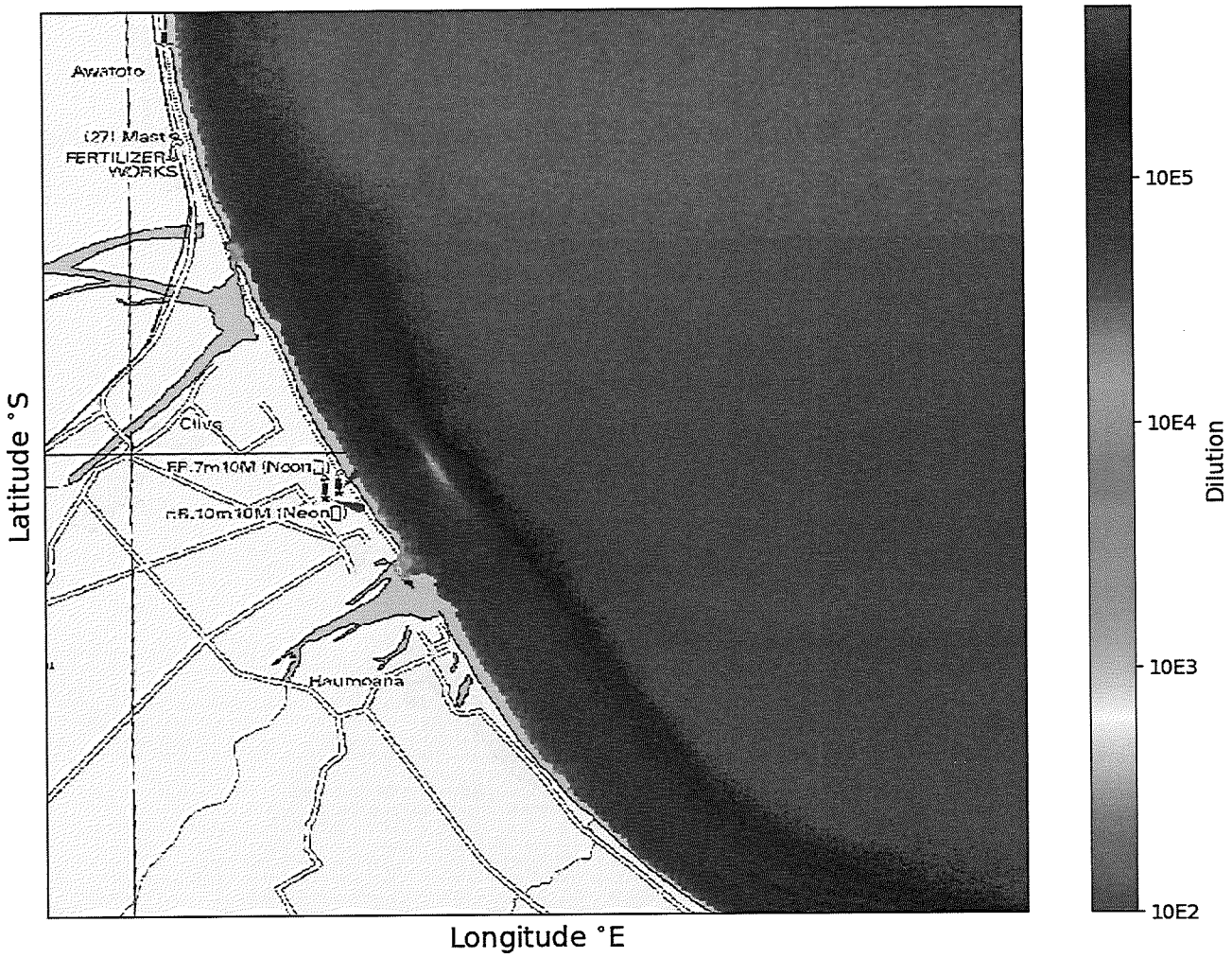

Figure A. 6 *Mean dilution during a month-long release at a rate of 48,000 m3 day-1 for a pipe break a quarter of the way along the pipe. Dilutions above 5.10^5 have been masked.*